

Computationally Intelligent Sensor System for Microwave Characterization of Dielectric Sheets

Satyajit Panda, Nilesh Kumar Tiwari, and Mohammad Jaleel Akhtar, *Senior Member, IEEE*

Abstract—An automated RF sensor system for accurate determination of complex permittivity of thin samples and dielectric sheets is proposed. The proposed system is computationally intelligent making use of the machine learning algorithm along with the artificial neural network (ANN) architecture and employs a coplanar waveguide sensor for the measurement of scattering coefficients of test specimens in order to obtain their dielectric properties. Different heuristics are followed for the design of the ANN-based system. The applicability of the proposed sensor system for practical usage is increased by taking into account the effect of possible air gap between the device and test specimen. This is facilitated by developing a multilayered analytical model, and combining it with the ANN-based system. The complete procedure, comprising of ANN algorithms and the analytical formulation, is implemented in MATLAB. The proposed automated standalone sensor system is validated by testing a number of standard samples in the designated frequency bands.

Index Terms—Artificial neural network (ANN), complex permittivity, curve fitting, coplanar waveguide, dielectric constant, loss tangent, machine learning (ML).

I. INTRODUCTION

NON-DESTRUCTIVE measurement of dielectric properties of materials in RF and microwave frequency bands is useful for a number of applications. In recent years, various resonant and non-resonant methods have been proposed for dielectric characterization of materials at RF and microwave frequencies [1]–[5]. Resonant methods are best known for their accuracy, but they have disadvantage of being narrow-band, and the test specimen should usually be machined in order to fit it inside the designed cavity.

For wide band RF characterization, a number of reflection only and reflection-transmission methods have been proposed in the literature. Many of the recent literatures focus on the complex permittivity determination of thin as well as layered material samples [1], [4]. Some methods [10], [11] employ reflection-only measurement setup for permittivity detection.

It has been shown that only reflection coefficient is not able to completely estimate the complex permittivity [12], [13], as it might lead to multiple solutions for the permittivity determination [14]. In order to obtain stable solution, the

transmission-reflection (T-R) approach appears to be a viable option [15], which actually provides quite satisfactory results. The reflection-transmission approach is conventionally being used for the rectangular waveguide geometry resulting into bulky measurement system.

It is to be noted that the open ended coaxial probe, which falls in the category of reflection only method, is commercially available and has gained importance for various industrial usage due to ease of measurement procedure. However, the coaxial probe is very bulky, which requires thick test samples and the procedure is also quite sensitive to even small air gap between the specimen and the probe. The coaxial probe is mostly used for liquid samples, as for solid samples the sample preparation is an issue. The coplanar waveguide (CPW) system, on the other hand can be used for both solids and liquids and it results into quite compact structure, which can be made portable and very easy procedure can be followed for measurement [6]–[9]. The coplanar waveguide structures are less dispersive than other geometries, and they are also having certain practical advantages as compared to other planar circuits because both the conductor and the ground planes are located on the upper surface of the substrate. It is mainly due to the above specified reasons that the CPW based sensor system is used here for microwave characterization. In this paper, the CPW is mainly used for characterizing of solid samples, but it can also be used for liquid samples with the help of a specially designed sample holder.

The determination of permittivity from scattering parameters is an inverse problem, which is generally solved using iterative methods. The iterative procedures require rigorous mathematical formulae and expressions to be solved, which may sometimes lead to convergence problems. These problems can be alleviated by the usage of computationally intelligent systems. The machine learning (ML) is one of the most acceptable techniques for making systems computationally intelligent. Artificial neural networks (ANN) can be used to perform various tasks such as prediction, clustering and classification, which are integral part of various ML algorithms. A number of neural network based approaches have been proposed in the past for characterization of liquid samples [10], [11]. One of these approaches uses a monopole antenna model to collect the data for network training [10]. The approach proposed in [11] employs an open ended coaxial probe for the sample placement and data acquisition. Both of these neural network based methods, however, use the non-planar structure and they have been specifically developed for characterizing liquid

Manuscript received June 22, 2016; accepted August 6, 2016. Date of publication August 12, 2016; date of current version September 16, 2016. The associate editor coordinating the review of this paper and approving it for publication was Dr. Richard T. Kouzes.

The authors are with the Department of Electrical Engineering, Indian Institute of Technology Kanpur, Kanpur 208016, India (e-mail: satyajitpanda020@gmail.com; nileshkt@iitk.ac.in; mjakhtar@iitk.ac.in).

Digital Object Identifier 10.1109/JSEN.2016.2599856

samples only.

Recently, a simple ANN based procedure was applied to a coplanar waveguide based system to characterize dielectric samples [17]. In this paper, the applicability of the overall procedure is increased further by refining the ANN algorithms, and a complete sensor system is proposed by considering the effect of possible air gap as well as the sample thickness. The coplanar waveguide system is used here as a sensor to collect the training data required for the proposed computationally intelligent system due to the advantages mentioned in the earlier paragraph. The proposed system is implemented using MATLAB to specifically characterize thin dielectric sheets. Although a single complex valued ANN architecture can be proposed by using CVNN (Complex Valued Neural Network), it results into severe complexity and poor convergence for the loss tangent. It is mainly due to this reason that four different real-valued ANNs with many performance improvements are implemented in this work. The neural network system requires a large and appropriate training dataset for efficient prediction of dielectric properties from the scattering parameters, which is collected here using the coplanar sensor as mentioned earlier [15]. The sensor system is simulated using the CST Microwave Studio (CST-MWS) [18] by considering a number of dielectric samples with their dielectric constant and loss tangent varying over a wide range. For faster learning, the cross entropy activation function is used in the hidden layers in lieu of the generic sigmoid function. Regularization methods are applied in the design to avoid over-fitting problem. Again the gradient descent algorithm with a momentum constant is used instead of the simple gradient descent approach because the later can get stuck in local minima problem. The performance of the proposed ANN architecture is estimated by plotting the error histogram and the regression. The measured scattering data for different known samples are obtained by placing them on the designed coplanar sensor. These data are then fed to the ANN system to determine the complex permittivity of these samples in the designated microwave frequency range, and the results are compared with their reference values.

One of the major problems of the planar RF sensors is the possible air gap between the device and the test specimen. A detailed sensitivity analysis is done here in order to critically observe the effect of air gap between the test sample and the CPW sensor, which also examines the effect of sample thickness variation. In this framework, an analytical multilayered model is also proposed to take into account the effect of air gap and to accordingly provide the appropriate correction factor. The analytical model is finally combined with the ANN algorithms to develop a computationally intelligent standalone system for microwave characterization of dielectric substrates and sheets. The proposed sensor system is tested and verified for various standard specimens using both simulated and the experimental data.

II. THEORY AND IMPLEMENTATION

A. Coplanar Waveguide Sensor

A multilayered conductor backed coplanar waveguide (MCCPW) is used here for the measurement

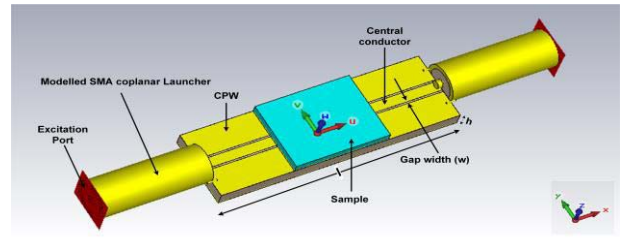


Fig. 1. CST simulation model of CPW sensor with samples.

of scattering parameters of test samples. The MCCPW sensor is simulated using the CST Microwave Studio [18] with the actual SMA-coplanar launchers connected at both the ends as shown in Fig. 1. It may be noted that in the past, the launchers were not taken into account in the simulation models which then required the de-embedding of the S-parameters from the launcher-plane to the CPW reference-plane [15]. This kind of simple de-embedding procedure quite often results into mismatch of the overall system thus degrading the overall accuracy and sensitivity of the measurement.

Hence the inclusion of launchers in the proposed simulated model provides good matching with the actual measurement system leading to accurate characterization of test specimens. All the simulations and measurements are carried out in the frequency range of 1-6 GHz, for which the sensor behaves quite efficiently. A large number of data sets are generated using the proposed CPW sensor setup shown in Fig. 1 by varying the dielectric properties of the test specimen over a wide range.

The CPW sensor is designed using the FR4 substrate with height (h) of 1.6 mm, length (l) of the line as 25.4 mm, the gap width (w) and the central conductor width (s) as 0.2 mm and 1.16 mm, respectively. The thickness of all the test samples is taken as 1 mm for the measurement and simulation purposes. The choice of taking 1 mm thick sample appears to be appropriate choice as justified in the later part of this paper after carrying out the sensitivity analysis.

B. ANN Modeling and Implementation

The method of permittivity determination in terms of the scattering coefficients is a non-linear inverse problem, for which the ANNs prove to work very efficiently. Here, several multilayer feed-forward neural networks in conjunction with EBPTA (Error Back Propagation Training Algorithm) are used to solve the corresponding inverse problem.

The ANN design is challenging due to the existence of a large number of physical architectures and learning algorithms, for a given non-linear problem. There exist many design variables, which must be determined carefully for optimal performance of the ANN. The multi-layer feed-forward ANN architecture used here comprises of multiple hidden layers along with one input and one output layer. The complexity of the neural network increases as the number of hidden layers increases. Similarly the number of neurons (perceptrons) also accounts for better result and also increases complexity. So the number of hidden layers and the neurons in each hidden layer should be chosen wisely. The choice of appropriate

input variables and bias values are critical and are chosen by repetitive error analysis of the ANN during training. Initially, the Gaussian random variables are assigned as weights of each neuron. During training these weights are updated by calculating the errors at the output stage and back propagating them to the hidden layers. For faster computation the Levenberg-Marquardt training algorithm is used, which is the fastest back-propagation algorithm and also requires less memory. The gradient descent function along with momentum constant is used to tackle the convergence issue. In this work, the learning rate, the momentum constant and the maximum number of epochs are chosen as 0.01, 0.9 and 1000, respectively after optimization. Since the dataset used is very large and random, the sigmoid activation function is not sufficient for the data fitting purpose. So the cross-entropy activation function is used for faster training of the network. Again to generalize the result beyond the training data, the activation function is upgraded by adding an extra regularization term. L2-regularization technique is used to alleviate the over-fitting problem. The regularized activation function used in the multi-layer ANN is represented as:

$$F = -\frac{1}{N} \sum_{x,j} y_j \log a_j^L + (1 - y_j) \log (1 - a_j^L) + \frac{\lambda}{2N} \sum_w w^2 \quad (1)$$

where ‘x’ represents the input, ‘y_j’ represents the desired output values of neuron and ‘a_j^L’ represents the actual output values. The parameter ‘λ’ is the regularization parameter and ‘N’ is the total number of training data. Similarly the output of a neuron is represented by the following equation:

$$Output = F \left(\sum_k (w_{j,k}^L * a_k^{L-1} + b_j^L) \right) \quad (2)$$

where ‘F’ represents the cross-entropy activation function with L2-regularization and ‘b’ represents the bias parameters. The BP (Back Propagation) algorithm is implemented in MATLAB rather than C as the former gives faster results [16].

Four BP networks are implemented in MATLAB for determination of the dielectric constant and the loss tangent. The specifications of the networks and the complete architecture are given in Table I and Fig. 2 respectively.

The network NA is used to calculate the dielectric constant, while NC and ND are used to calculate the loss tangent of materials. The network NB employs an improved algorithm to categorize the materials on the basis of their loss tangent value.

A 5-tuple vector, Input = [frequency, Re (S₁₁), Im (S₁₁), Re (S₂₁), Im (S₂₁)] is fed to the input layer and a single output is taken from the output layer. The measured data in touchstone format are imported from the vector network analyzer (VNA) into MATLAB for the permittivity determination as shown in Fig. 2.

C. Multilayered Analytical Model for Air Gap Correction

There may be some air gap between the test specimen and the designed coplanar sensor during measurement due to

TABLE I
NEURAL NETWORK SPECIFICATION

ANN	Size of Training Data (Rows)	No. of neurons in hidden layer-1 (n1)	No. of neurons in hidden layer-2 (n2)	Function of the ANN
NA	60*51	100	-	Determination of real part of the permittivity
NB	49*51	75	-	Categorize data into high and low loss samples
NC	47*51	50	25	Determination of loss tangent of high loss samples
ND	60*51	100	70	Determination of loss tangent of low loss samples

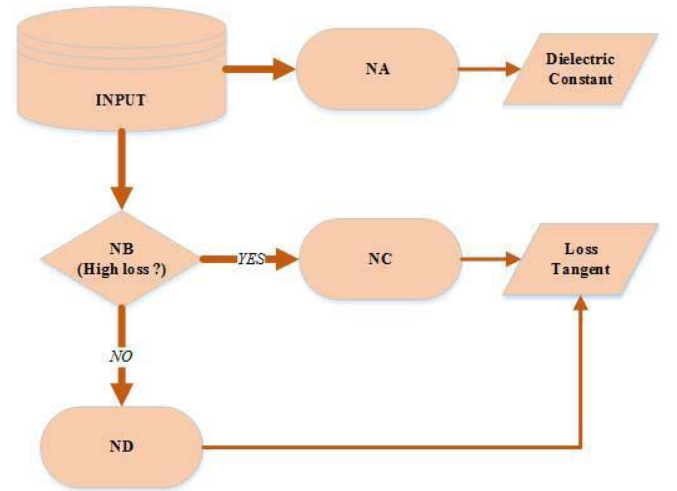


Fig. 2. The proposed neural network architecture.

imperfect machining of samples. The air gap might be non-uniform, which can be effectively modeled as a uniform air gap between the sample and the sensor, averaged over entire surface of the sample, using the procedure described later in the text.

It is to be noted that the neural network program is not able to accurately estimate the loss tangent of test samples under situations where air gap is present. Hence, the analytical models are proposed here to model the possible air-gap present between the device and the test specimen in order to determine the approximate value of the dielectric constant and the loss tangent of the test specimen. The obtained loss tangent of the test specimen under air-gap situation is further refined with the help of optimization algorithm as described in the later part of the text.

A three layered coplanar waveguide model is already available in literature [7], but this model cannot take into account

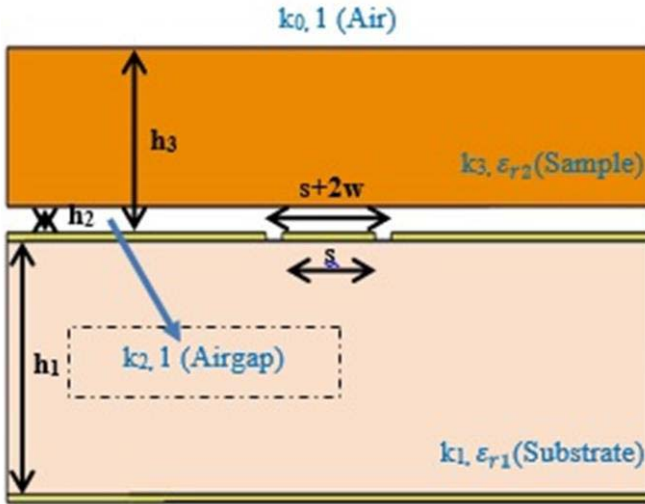


Fig. 3. Schematic of the MCCPW with air gap and sample.

the effect of air gap during measurement. In this paper, a four layered model for the conductor backed coplanar waveguide is proposed to consider the effect of air gap between the test sample and the sensor.

1) *The Exact Four Layered Model:* Fig. 3 shows the cross-sectional schematic of the four layered (Substrate-Air gap-Sample-Air) MCCPW structure. The effective complex permittivity of the whole system can be calculated from the scattering parameters using T-R method [15] as given by following equations (3)–(6).

$$Y = \frac{1 + S_{21}^2 - S_{11}^2}{S_{21}} \quad (3)$$

$$t = \frac{Y}{2} \pm \sqrt{\left(\frac{Y}{2}\right)^2 - 1} \quad (4)$$

$$\gamma = \frac{\ln |1/t|}{l} + \left(\frac{\arg(1/t) + 2n\pi}{l}\right) i \quad (5)$$

$$\varepsilon_{r,eff} = -\left(\frac{\gamma}{\gamma_0}\right)^2 \quad (6)$$

where l is the length of the sample, γ and γ_0 are the overall propagation constants of the medium and air respectively, and $\varepsilon_{r,eff}$ represents the effective complex permittivity of the CPW-sensor system.

The expressions for $\varepsilon_{r,eff}$ also can be derived from the multilayered CPW model shown in Fig. 3, by applying conformal mapping procedure.

$$\varepsilon_{r,eff} = \frac{\{(\varepsilon_{r1} - 1) \frac{K(k_1)}{K(k'_1)} + (1 - \varepsilon_{r2}) \frac{K(k_2)}{K(k'_2)} + (\varepsilon_{r2} - 1) \frac{K(k_3)}{K(k'_3)} + \frac{K(k_0)}{K(k'_0)} + \frac{K(k_1)}{K(k'_1)}\}}{\frac{K(k_0)}{K(k'_0)} + \frac{K(k_1)}{K(k'_1)}} \quad (7)$$

Here ε_{r1} and ε_{r2} are the relative permittivity of the substrate (known) and the test sample (to be calculated), respectively. The symbols $K(\cdot)$ and $K(\cdot')$ represent the complete elliptic

integral of first kind and its complement respectively. The argument of the elliptic integrals for the different layers of the MCCPW model (k_i) are governed by the following equations (8)–(11).

$$k_0 = \frac{s}{s + 2w} = \frac{a}{b} \quad (8)$$

$$k_1 = \frac{\tanh(\pi s/4h_1)}{\tanh(\pi(s + 2w)/4h_1)} \quad (9)$$

$$k_2 = \frac{\sinh(\pi s/4h_2)}{\sinh(\pi(s + 2w)/4h_2)} \quad (10)$$

$$k_3 = \frac{\sinh(\pi s/4h_3)}{\sinh(\pi(s + 2w)/4h_3)} \quad (11)$$

The complete elliptic integrals are very well known special type of integrals, whose closed form expression is given by the equation:

$$\frac{K(k_i)}{K(k'_i)} = \begin{cases} \frac{\pi}{\ln \left[\frac{2(1 + \sqrt{k'_i})}{(1 - \sqrt{k'_i})} \right]}; & 0 \leq k_i \leq 0.707 \\ \frac{1}{\pi} \ln \left[\frac{2(1 + \sqrt{k_i})}{(1 - \sqrt{k_i})} \right]; & 0.707 \leq k_i \leq 1 \end{cases} \quad (12)$$

where k'_i can be expressed as $k'_i = \sqrt{1 - k_i^2}$.

After calculating the complete elliptic integrals for all the four layers of the model, they can be substituted in (7) to calculate the permittivity of the test sample (ε_{r2}).

2) *The Approximated Three Layered Model:* The field of the coplanar sensor is concentrated mostly near the substrate and decays quite fast as we move away from it towards the sample-air interface. Due to the above fact, the sample thickness for even moderately thin specimens can be approximated to be large or all practical purposes, which reduces our model to a three layered model (Substrate-Air gap-Sample) by making $h_3 \rightarrow \infty$ in Fig. 3. The conformal mapping relations, developed from the capacitance model are governed by the equations (13)–(15). The symbols $\varepsilon'_{(\cdot)}$, $\varepsilon''_{(\cdot)}$ and $\tan \delta_{(\cdot)}$ represent the dielectric constant, the loss factor and loss tangent of the material, respectively, with the complex permittivity as ($\varepsilon_{(\cdot)} = \varepsilon'_{(\cdot)} - i\varepsilon''_{(\cdot)}$). Solving equations (13), (14) and

$$\varepsilon'_{r,eff} = q_1 \varepsilon'_{r1} + q_2 + q_3 \varepsilon'_{r2} \quad (13)$$

$$\varepsilon''_{r,eff} = q_1 \varepsilon''_{r1} + q_3 \varepsilon''_{r2} \quad (14)$$

$$\tan \delta_i = \frac{\varepsilon''_{ri}}{\varepsilon'_{ri}} \quad (15)$$

(15) simultaneously, we can get a relation between effective loss tangent and the loss tangent of the sample (to be calculated) as follows:

$$\tan \delta_{eff} = q_1 \frac{\varepsilon'_{r1}}{\varepsilon'_{r,eff}} \tan \delta_1 + q_3 \frac{\varepsilon'_{r2}}{\varepsilon'_{r,eff}} \tan \delta_2 \quad (16)$$

Once the filling factors (q_i) for all the three layers are known, the unknown dielectric constant (ε'_2) and loss tangent ($\tan \delta_2$) of the dielectric sample can be calculated from (13) and (16) respectively, as other variables used in

TABLE II
COMPARISON OF MEASURED RESULTS

Method	Reference values of the specimen [19]-[23]		Measured data (Averaged over 1-6GHz and for five set of measurements)		Percentage error	
	ϵ'_r	$\tan\delta$	ϵ'_r	$\tan\delta$	$\%\epsilon'_r$	$\%\tan\delta$
FR4	4.3	0.025	4.3012	0.0247	0.03	1.2
Epoxy-Resin	3.5	0.06	3.6552	0.0573	4.43	4.5
Plexiglass	3.4	0.001	3.4460	0.0011	1.35	10
PVC	3.0	----	3.1001	0.0123	3.33	----
Rubber	3.0	----	3.0483	0.0048	1.61	----
Poly-styrene	2.6	0.00033	2.6506	0.00035	5.0	5.71
Poly-Ethylene	2.26	0.00031	2.2640	0.00029	0.18	6.45
Teflon	2.1	0.00028	2.1003	0.00026	0.01	7.14

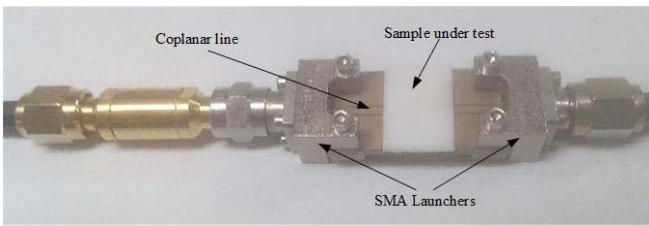


Fig. 4. Measurement Setup (MCCPW with sample placed on it).

these expressions are known for a designed coplanar sensor. The filling factors (q_i) for different layers of the MCCPW can be calculated using the relatively simpler expressions given below.

$$q_1 = \frac{\frac{K(k_1)}{K(k'_1)}}{\frac{K(k_0)}{K(k'_0)} + \frac{K(k_1)}{K(k'_1)}} \quad (17)$$

$$q_2 = \frac{\frac{K(k_2)}{K(k'_2)}}{\frac{K(k_0)}{K(k'_0)} + \frac{K(k_1)}{K(k'_1)}} \quad (18)$$

$$q_3 = 1 - q_1 - q_2 \quad (19)$$

The above approximated model facilitates simpler calculations than the exact model for determination of complex permittivity of samples in most of the situations, and matches with the later in the limiting case.

III. MEASUREMENT RESULTS AND DISCUSSION

The design of the neural networks is incomplete without proper training. All the four networks are trained with sufficiently large and relevant data sets. Proper training is ensured by performance evaluation of the trained neural networks using the regression analysis and plotting the error histograms in MATLAB.

The designed neural networks are validated by taking the measurement data of unloaded MCCPW sensor, and by loading the sensor with several reference samples (Teflon, Poly-Ethylene, PVC, FR4, Poly-styrene, Plexiglass, Rubber and Epoxy-resin) having known complex permittivity values. The thickness of all the samples is taken to be 1 mm, and the samples are placed on the CPW sensor as shown

in Fig. 4. The CPW sensor is connected to the vector network analyzer through coaxial SMA launchers. The experiment was carried out in normal room temperature conditions. To avoid the uncertainty in experimental results, the measurements are repeated five times with five different calibration sets for each of the eight samples and the results are averaged to get the final value (listed in fourth and fifth columns of Table II). All the measurements are performed using the PNA-series Agilent N5230C network analyzer. The Agilent 85052D CALIBRATION KIT is used for the short-open-load-through (SOLT) calibration. After calibration, the scattering parameters of the available materials are recorded in the desired frequency range (1 to 6 GHz) and saved in the touchstone file format.

These touchstone files are then fed to the machine learning algorithm developed in MATLAB for determination of the complex permittivity. The detailed architecture and the functionality of the neural nets have already been explained in section-II (B). After successful training of all the four neural networks, the network A (NA) is used for calculation of the dielectric constant. Then the same data is transferred to network B (NB), which categorizes the data into two categories by analyzing the patterns in the data. The network NB has the basic functionality to decide whether the material has high or low loss factor. If the loss tangent lies between 0.0001 and 0.01, then the sample is considered as low loss material, and if it is more than 0.01, the sample is considered as high loss material. Then the algorithm channels the data automatically to network C (NC) or network D (ND), depending on whether the sample is of high loss or low loss category respectively, for calculating the loss tangent accurately. It is to be noted that this category division is done to achieve better sensitivity of the neural networks NC and ND for the determination of loss tangent.

The complex permittivity determined by the proposed ANN based system for all the aforementioned samples are shown in Fig. 5 and Fig. 6(a) and (b). The measurement results are compared with the data of these samples available in the literature [19]-[23] and are also listed in Table II.

The retrieved dielectric constants of test samples (averaged over five set of measurements), which are calculated using the network NA are shown in Fig. 5. The network B categorized

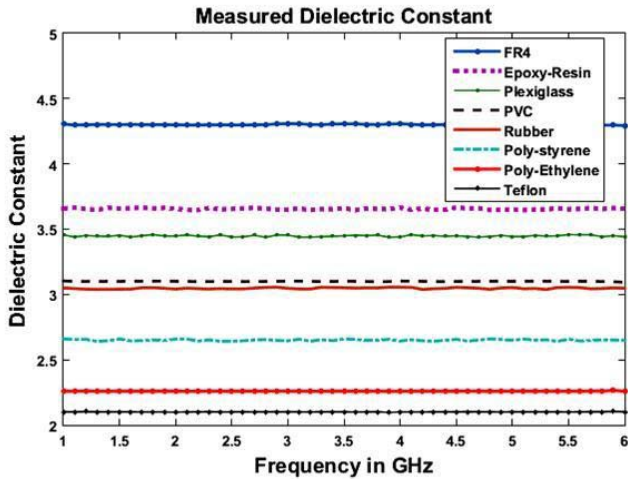


Fig. 5. Measured dielectric constant for various test samples.

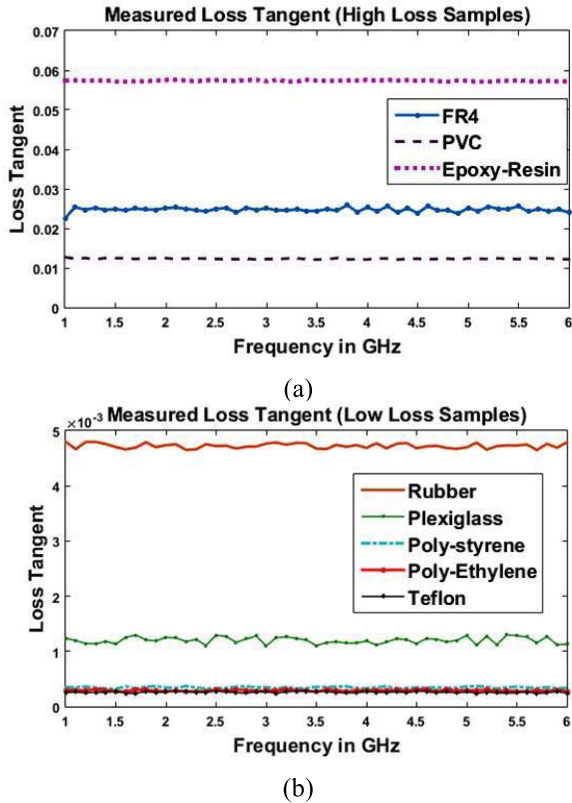


Fig. 6. Measured loss tangent ($\tan\delta$) for various test samples. (a) High loss samples. (b) Low loss samples.

PVC, FR4 and Epoxy-resin samples as high loss materials, and rest five of the eight samples as low loss materials based on the criterion discussed earlier. The scattering data are then accordingly fed into respective networks for the loss tangent determination. The calculated loss tangent (averaged over five set of measurements) in the designated frequency range are plotted in Fig. 6(a) and (b) categorically, for high loss and low loss samples respectively.

The complex permittivity (dielectric constant and loss tangent) data retrieved from the measurement for the given

TABLE III
DIELECTRIC TESTING OF SOME NON-STANDARD MATERIALS

Material	Measured Data (Averaged over 1-6 GHz)	
	ϵ'_r	ϵ''_r
Brick	3.9593	0.0263
Concrete	4.4951	0.0735
Gavel	8.8176	0.0534
Green Marble	5.4671	0.0188
Carrot	30.5147	0.2910
Potato	36.8991	0.3477

samples are compared with their values available in literatures [19]–[23] as given in columns 2 and 3 of Table II. The measured dielectric properties of the samples (averaged over five set of measurements) using the fabricated MCCPW sensor are given in 4th and 5th columns of Table II. The percentage errors in the retrieved dielectric data for these samples are calculated and listed in the columns 6 and 7 of Table II. It can be concluded from Table II that the retrieved complex permittivity using the proposed CPW-machine learning algorithm is in good agreement with the standard values available in the literature. It also shows that the dielectric constant and the loss tangent measurement are possible with a typical error margin of 5% and 10%, respectively.

It is verified from Table II that the system works fine for materials with moderate and high dielectric losses. However, for very low loss materials like Teflon, Poly-Ethylene and Poly-styrene it predicts the loss tangent with somewhat lower accuracy. The reason behind this is that most of the transmission line based methods have difficulty in retrieving the loss tangent values of very low loss samples due to limitation of scattering parameter measurement.

After successful evaluation of the ANN based system against the standard samples with known permittivity values, the system is used to test some naturally available materials, whose dielectric properties are unknown. Some stone like samples (gravel, concrete, brick and green-marble) and two vegetable samples (potato and carrot) are accordingly measured and the results are tabulated in Table III to give a quantitative measure. It should be noted that fresh potato and carrot samples are used here for the measurement.

Meanwhile, the error listed in columns 6 and 7 of Table II can be attributed to number of factors such as variation of the thickness of the fabricated samples from the value that is used for measurement and possible air gap between the CPW sensor and the fabricated sample. Sensitivity analysis is discussed in next section, and accordingly necessary correction factors are proposed to minimize the error.

IV. SENSITIVITY ANALYSIS

The samples used for the measurement purpose are machined carefully in order to get a very flat and smoothed surface so that they can be placed on the designed sensor with good precision. However, some time it is quite difficult to make the test specimen to be quite flattened, and hence there might be some unwanted air gap between the device and the

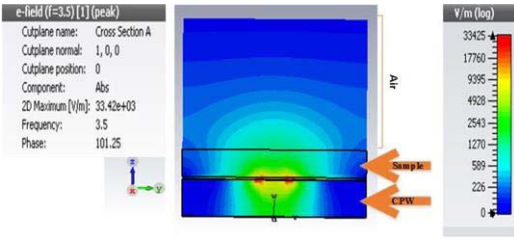


Fig. 7. Cross-sectional electric field pattern of the MCCPW sensor.

TABLE IV
EFFECT OF AIR GAP VARIATION

Sample	Air gap(mm)	Error in ϵ_r	Error in $\tan\delta$
FR4	0	0%	0%
Teflon		0%	0%
FR4	0.01	3.13%	0.8%
Teflon		2.13%	2.22%
FR4	0.02	4.79%	1.62%
Teflon		4.28%	2.39%
FR4	0.03	11%	6.94%
Teflon		9.28%	2.8%
FR4	0.05	22.97%	8.76%
Teflon		18.26%	3.04%

test specimen, which may lead to inaccurate measurements. Similarly, the variation in thickness of the samples also can have impact on the experimental results especially for very thin samples. Hence, the sensitivity analysis of the designed measurement system to the take into account the effect of these two factors is carried out in this section.

A. Effect of Air Gap Variation

The air gap is a very common problem in dealing with any kind of planar device for EM measurement of solid samples. The electric field pattern of the MCCPW is shown in Fig. 7. From this figure, it is clearly visible that the electric field is concentrated near the surface of the CPW. The fields are having maximum value near the surface and decay rapidly as one moves outwards towards the sample-air interface. It basically means that even small air gap between the surface of the CPW sensor and the test specimen, if present, can significantly affect the dielectric measurement result. To quantify the effect of air gap in the proposed system, the scattering data are recorded for two samples FR4 and Teflon with different air gaps, and the percentage error in the predicted dielectric constant and loss tangent are tabulated in Table IV.

It can be observed from Table IV that when the air gap varies from 0 to 0.05 mm, the error in both dielectric constant and loss tangent increases. When the air gap is less than 0.02 mm, then the computed error is within tolerable limit of 5%. However, if the air gap increases beyond 0.02 mm for a given sample, the error in both the dielectric constant and the loss tangent starts increases a very higher rate. Hence, it can be postulated that some kind of air gap correction must be applied under situations when the air gap

TABLE V
EFFECT OF SAMPLE THICKNESS VARIATION

Sample	Thickness(mm)	Error in ϵ_r	Error in $\tan\delta$
FR4	1.5	1.03%	0.43%
Teflon		0.9%	0.27%
FR4	1	0%	0%
Teflon		0%	0%
FR4	0.6	4.88%	4.04%
Teflon		4.24%	1.59%
FR4	0.5	10.48%	4.45%
Teflon		6.44%	3.87%
FR4	0.3	21.6%	6.15%
Teflon		13.97%	5.17%

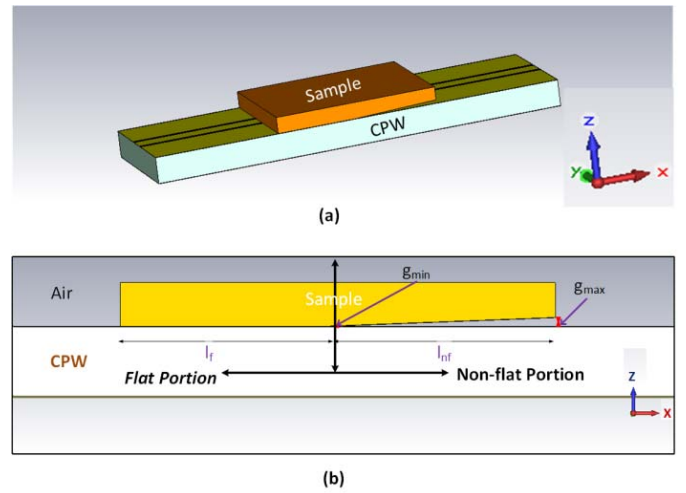


Fig. 8. The geometry of a non-flat sample showing air gap. (a) Perspective view. (b) Cross-sectional view.

between the test specimen and the designed sensor increased beyond 0.02 mm.

B. Effect of Sample Thickness Variation

For observing the effect of the sample thickness on the measurement, several readings are taken for two samples, FR4 and Teflon with different thickness values. The dielectric constant and the loss tangent data are derived using the proposed algorithm, and the percentage error in the calculation of dielectric constant and loss tangent are tabulated in Table V. It is observed that if the thickness varies from 1 mm down to 0.3 mm, the error percentage increases monotonically. Looking at the error profile, it can be noticed that the change in the error is smooth until a sample thickness of 0.6 mm. For sample of thickness less than 0.6 mm, the error starts increasing very rapidly. However, when the sample thickness is increased above 1 mm, then the change in the dielectric values is not that significant as seen from Table V. So allowing an error threshold of 5% in the dielectric constant and loss tangent, the test sample must have a minimum thickness of 0.6 mm.

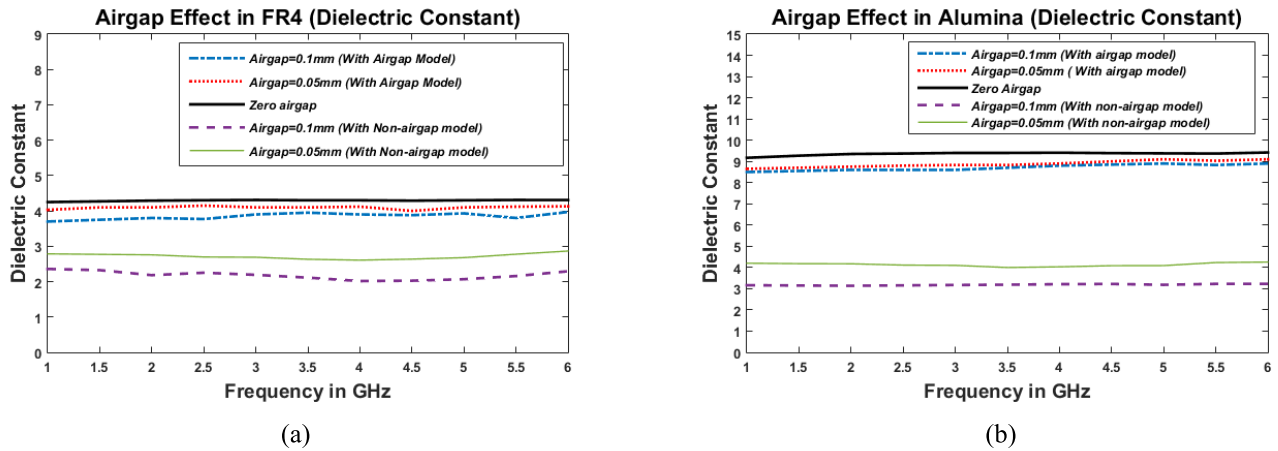


Fig. 9. Effect of air gap in dielectric constant of different samples with air gap and non-air gap models. (a) FR4. (b) Alumina.

C. Air Gap Calibration

The sensitivity analysis done in the previous section is based on the assumption that the air gap is uniform. But practically it can't be uniform as the sample may have non-flat surface due to improper machining. It will be very difficult to analyze and apply correction for the non-uniform air gap. So in this section a manual calibration technique is proposed to convert the non-uniform air gap into a uniform one, so that the correction will be easier.

As the sample is rectangular in shape, there are two possibilities of non-flatness. One possibility is that the sample is not flat along the length of the coplanar line (x -direction in Fig. 8), and the other option is that there is non-flatness along the width (y -direction in Fig. 8). But the geometry of the CPW sensor ensures that most of the fields are concentrated along the central metal strip, due to which the air gap due to the broadside non-flatness doesn't affect the measurement result. So our main concern here is to analyze the case where the air gap primarily exists along the central conductor as shown in Fig. 8. The sample has some part (l_f) in contact with the CPW substrate, whereas some portion (l_{nf}) is elevated due to non-flatness and produces some air gap. As the air gap is considered to be small (of the order of tens/hundreds of microns) the non-flat surface can be approximated to be linear with a constant slope. So the average air gap can be approximated as $g = g_{avg} = (g_{min} + g_{max})/2$ over the non-flat portion of the surface (l_{nf}), where g_{min} and g_{max} are the minimum and maximum air gap in the non-flat region. The effective portion of the sample which is having some air gap is given by the calibration factor, $f_{cal} = l_{nf}/(l_f + l_{nf})$. So the effective air gap over the whole sample can be calculated as $g_{eff} = g_{avg} * f_{cal}$. This calibration is manual and can be done with a little effort provided that the maximum and minimum air gap can be measured accurately.

D. Air Gap Correction

As per discussions in the previous two subsections, it is clear that the effect of sample thickness is not quite significant if a specimen of more than 0.6 mm thickness is chosen for

measurement. However, the effect of air gap is more severe as even air gap of more than 0.02 mm can provide quite erroneous result during measurement. It is quite difficult to obtain quite flat samples practically and hence a small air gap is sometimes unavoidable. Hence, some correction factor must be applied to take into account the effect of the air gap during measurement.

In this work, a feed-forward neural network with three hidden layers is designed for calculation of the dielectric constant taking into account the air gap effect. This neural network has an extra training parameter i.e., the air gap in addition to the 5-tuple vectors which have been used earlier for modeling situation without any air gap. A total of 200 samples are simulated in CST-MWS [18] for the training dataset. This neural network, after being successfully trained, is able to predict the dielectric constant with accepted level of accuracy. But the neural network approach becomes too complicated to predict the loss tangent accurately due to highly nonlinear dataset.

The multilayered analytical model proposed earlier in this paper has then been used to approximately compute the loss tangent as well as the dielectric constant in these situations. The proposed multilayered analytical model is able to calculate the dielectric constant of samples with a satisfactory accuracy for different values of air gaps. But it is not able to find the loss tangent very accurately. So after getting the coarse initial guess of the dielectric properties using the proposed analytical model, the optimization algorithm is employed here for accurate loss tangent determination. The in-built routines of the CST-MWS [18] are used for the optimization purpose. The optimized algorithm is verified by considering various known samples with different air gaps. Some of these observations are shown in Fig. 9 and Fig. 10. Fig. 9(a) and (b) show the dielectric constant data of FR4 and Alumina, respectively calculated with and without considering the effect of air gap. It clearly shows that if the dielectric values are computed without air gap model, then there is significant amount of error between the actual and the estimated values. After finding the dielectric constant, the air gap analytical model is first used to calculate the loss tangent. These values are not

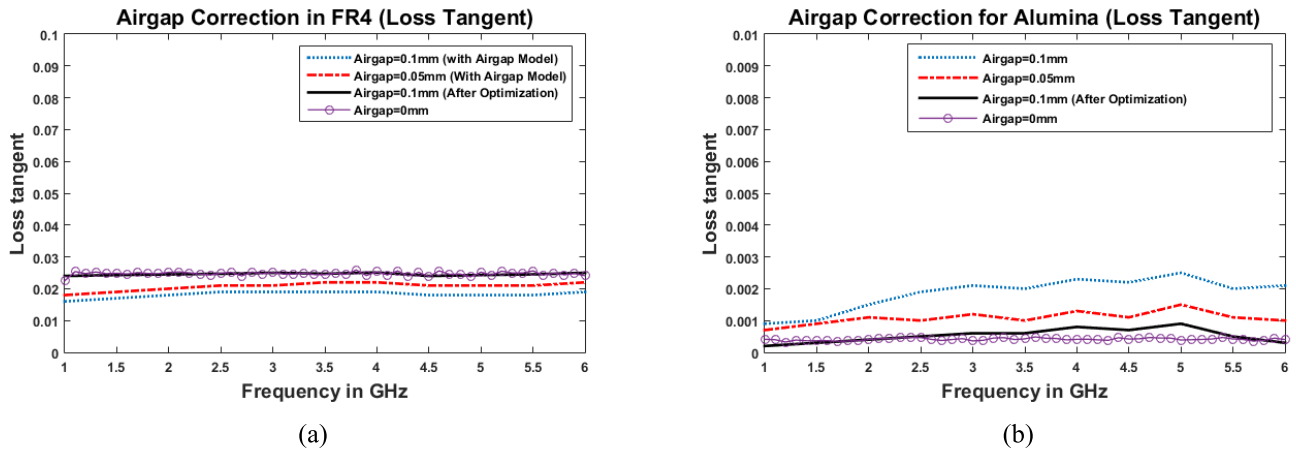


Fig. 10. Effect of air gap in the loss tangent of samples with different air gap and its corrected value after optimization. (a) FR4. (b) Alumina.

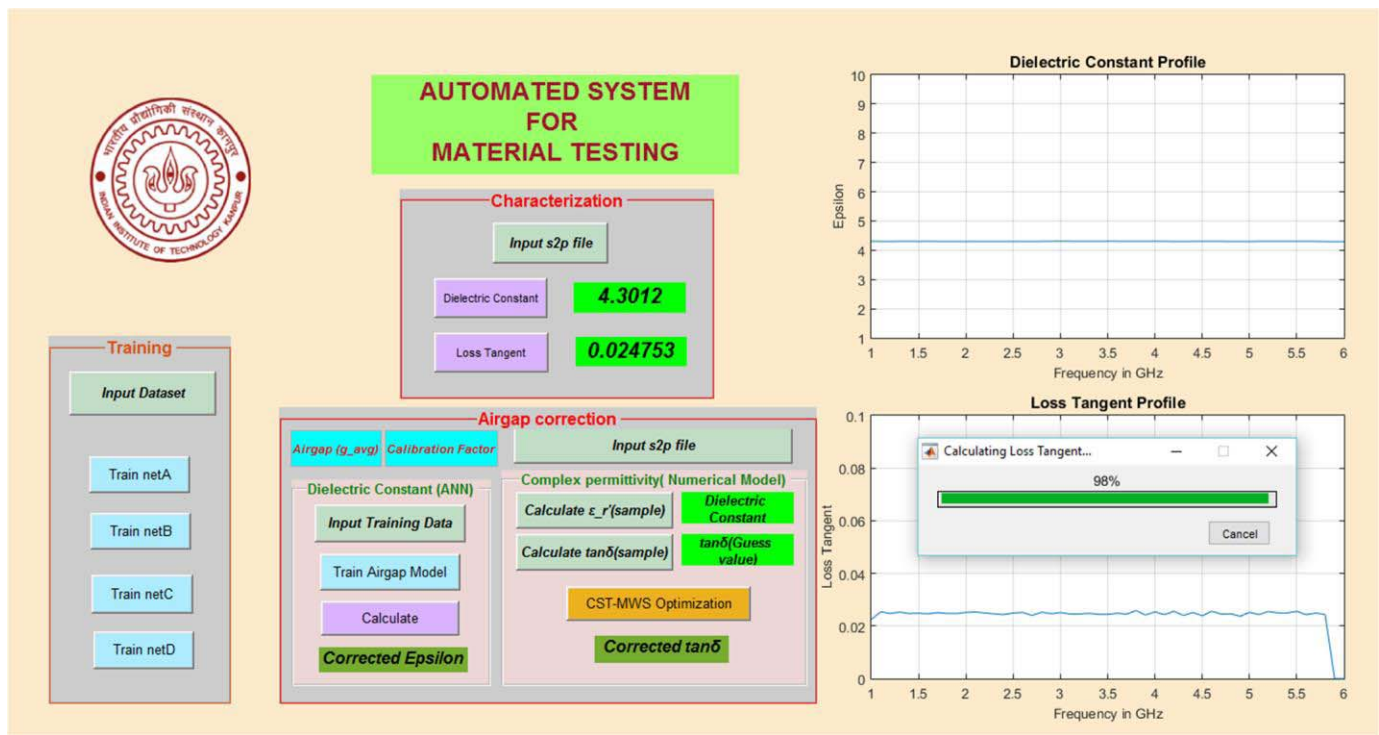


Fig. 11. The intelligent automated system for material characterization (calculating the permittivity profile of FR4 sample).

quite accurate, and hence they are further refined using the optimization procedure. The optimized loss tangent data using the CST-MWS optimizer module are also shown in Fig. 10 for both the above-specified samples, which obviously have much higher accuracy. From the above discussion, it is clear that the proposed multi-layered analytical model of the CPW sensor along with the CST [18] based optimization algorithm can be used to characterize samples under situation where some air gap is available between the device and the test specimen.

V. THE INTELLIGENT STANDALONE APPLICATION FOR MATERIAL CHARACTERIZATION

Using the concepts discussed above, an automated RF sensor system is designed using the MATLAB graphical

user interface. The designed system is a standalone application and can be run on systems without having MATLAB. The graphical user interface for the developed application is shown in Fig. 11.

The application has three major modules namely ‘Training’, ‘Characterization’ and ‘Air gap Correction’. The first two modules are assigned to the determination of the complex permittivity of the samples if there is no air gap. These two modules are thus interdependent. The first module does the task of training the designed neural networks (NA, NB, NC and ND). During training the performance analysis can be done to check whether the training is successful or not. As mentioned earlier only after successful training, the neural networks are ready for measurement of dielectric properties

of materials. After proper training, the module 2 (Characterization) can be used for determination of the dielectric constant as well as the loss tangent of test specimens. This module also has two axes extensions to plot the material properties viz., the dielectric constant and the loss tangent profile dynamically. The input dataset required by these two modules can be provided via the pushbuttons which direct the user to select the data files interactively.

The third module is devoted towards the air gap correction, which is applicable for samples which are not very flat, and hence some air gap remains between the specimen and the CPW sensor. This module has two sub-modules, out of which any one can be selected by the user depending upon the requirement. The first one should be used when only dielectric constant is required. When the user requires both the dielectric constant and the loss tangent of specimens with the presence of air gap, the second sub-module should be chosen for measurement.

VI. CONCLUSION

A complete intelligent RF system has been designed and developed for the characterization of thin dielectric sheets using the concept of machine learning. A standalone application has been developed by integrating all the procedures using the MATLAB graphical user interface. The machine learning algorithm uses the state of the art artificial neural networks, which are used to realize nonlinear mathematical functions, as the characterization is a nonlinear inverse problem. The proposed system is able to determine the complex permittivity of test specimens in the microwave frequency range of 1-6 GHz with a good accuracy. In order to maintain consistency in the results, repetitive measurements are performed for each sample and variations in the results are averaged out. There is a scope for further improvement in the accuracy especially for very low loss materials by using deep learning ANNs at the cost of complexity. The effect of the air gap (due to improper machining), if present between the sample and the device, during measurement has been addressed in this paper both qualitatively as well as quantitatively. The overall CPW measurement system has been automated by the use of machine learning algorithm, which reduces the time taken by the complex iterative procedures. Our main focus here has been the characterization of solid dielectric sample, but with some minor modifications, the developed system can also be used for characterization of liquid samples. Further, the overall approach can be extended for determination of magnetic properties of materials (e.g. permeability), as well as for characterization of concretes and other NDE (Non Destructive Evaluation) based systems.

REFERENCES

- [1] U. C. Hasar, "Accurate complex permittivity inversion from measurements of a sample partially filling a waveguide aperture," *IEEE Trans. Microw. Theory Techn.*, vol. 58, no. 2, pp. 451–457, Feb. 2010.
- [2] M. M. Scott and D. L. Faircloth, "Microwave permittivity determination for materials with out-of-plane and off-diagonal dielectric anisotropy," *IEEE Trans. Microw. Theory Techn.*, vol. 61, no. 6, pp. 2471–2480, Jun. 2013.
- [3] A. Aydoğan and F. Akleman, "Analysis of direct and inverse problems related to circular waveguides loaded with inhomogeneous lossy dielectric objects," *IEEE Trans. Microw. Theory Techn.*, vol. 62, no. 6, pp. 1291–1300, Jun. 2014.
- [4] M. S. B. A. Karim, Y. Konishi, K. Harafuji, and T. Kitazawa, "Determination of complex permittivities of layered materials using waveguide measurements," *IEEE Trans. Microw. Theory Techn.*, vol. 62, no. 9, pp. 2140–2148, Sep. 2014.
- [5] T. Yilmaz, R. Foster, and Y. Hao, "Towards accurate dielectric property retrieval of biological tissues for blood glucose monitoring," *IEEE Trans. Microw. Theory Techn.*, vol. 62, no. 12, pp. 3193–3204, Dec. 2014.
- [6] A. Raj, W. S. Holmes, and S. R. Judah, "Wide bandwidth measurement of complex permittivity of liquids using coplanar lines," *IEEE Trans. Instrum. Meas.*, vol. 50, no. 4, pp. 905–909, Aug. 2001.
- [7] B. Kang, J. Cho, C. Cheon, and Y. Kwon, "Nondestructive measurement of complex permittivity and permeability using multilayered coplanar waveguide structures," *IEEE Microw. Wireless Compon. Lett.*, vol. 15, no. 5, pp. 381–383, May 2005.
- [8] C.-S. Lee and C.-L. Yang, "Thickness and permittivity measurement in multi-layered dielectric structures using complementary split-ring resonators," *IEEE Sensors J.*, vol. 14, no. 3, pp. 695–700, Mar. 2014.
- [9] M. A. H. Ansari, A. K. Jha, and M. J. Akhtar, "Design and application of the CSRR-based planar sensor for noninvasive measurement of complex permittivity," *IEEE Sensors J.*, vol. 15, no. 12, pp. 7181–7189, Dec. 2015.
- [10] A. Hasan and A. F. Peterson, "Improved measurement of complex permittivity using artificial neural networks with scaled inputs," *Microw. Opt. Technol. Lett.*, vol. 53, no. 9, pp. 2139–2142, Sep. 2011.
- [11] Q. Chen, K.-M. Huang, X. Yang, M. Luo, and H. Zhu, "An artificial neural network realization in the measurement of material permittivity," *Prog. Electromagn. Res.*, vol. 116, pp. 347–361, 2011.
- [12] U. C. Hasar and C. R. Westgate, "A broadband and stable method for unique complex permittivity determination of low-loss materials," *IEEE Trans. Microw. Theory Techn.*, vol. 57, no. 2, pp. 471–477, Feb. 2009.
- [13] O. Büyükköztürk, T.-Y. Yu, and J. A. Ortega, "A methodology for determining complex permittivity of construction materials based on transmission-only coherent, wide-bandwidth free-space measurements," *Cement Concrete Compos.*, vol. 28, no. 4, pp. 349–359, Apr. 2006.
- [14] V. V. Varadan and R. Ro, "Unique retrieval of complex permittivity and permeability of dispersive materials from reflection and transmitted fields by enforcing causality," *IEEE Trans. Microw. Theory Techn.*, vol. 55, no. 10, pp. 2224–2230, Oct. 2007.
- [15] M. S. Shete, M. Shaji, and M. J. Akhtar, "Design of a coplanar sensor for RF characterization of thin dielectric samples," *IEEE Sensors J.*, vol. 13, no. 12, pp. 4706–4715, Dec. 2013.
- [16] J. Nazari and O. K. Ersoy, "Implementation of back-propagation neural networks with MATLAB," Dept. Elect. Comput. Eng., Purdue Univ., West Lafayette, IN, USA, Tech. Rep. 275, 1992.
- [17] S. Panda, N. K. Tiwari, and M. J. Akhtar, "Neural network based system for RF testing of thin samples," in *Proc. IEEE MTT-S Int. Microw. RF Conf. (IMARC)*, Hyderabad, India, Dec. 2015, pp. 230–233.
- [18] (2015). *CST-Computer Simulation Technology*. [Online]. Available: <http://www.cst.com>
- [19] M. J. Akhtar, L. Feher, and M. Thumm, "Measurement of dielectric constant and loss tangent of epoxy resins using a waveguide approach," in *Proc. IEEE Antennas Propag. Soc. Int. Symp.*, Albuquerque, NM, USA, Jul. 2006, pp. 3179–3182.
- [20] RF Cafe. (May 12, 2016). *Dielectric Constant, Strength and Loss Tangent*. [Online]. Available: <http://www.rfcafe.com/references/electrical/dielectric-constants-strengths.htm>
- [21] The Engineering Toolbox. (May 12, 2016). *Relative Permittivity-Dielectric Constant*. [Online]. Available: http://www.engineeringtoolbox.com/relative-permittivity-d_1660.html
- [22] Best Electronic Materials for 3-6 GHz Designs. (Mar. 16, 2016). *Best Materials for 3-6 GHz DESIGN*. [Online]. Available: <http://www.parkelectro.com/parkelectro/images/leysfinal.pdf>
- [23] PedaSoft's Online User Guide. (May 12, 2016). *Dielectric Constant and Loss Tangent*. [Online]. Available: http://www.pedasoft.com/dielectric_constant_and_loss_tangent.htm



Satyajit Panda received the M.Tech. degree in electrical engineering from the Indian Institute of Technology Kanpur, Kanpur, India, in 2016. His current research interests include machine learning, microwave characterization, and microwave non-destructive testing.



Nilesh Kumar Tiwari received the B.E. degree in electronics and communication engineering from RGPV University Bhopal, India, in 2007. He is currently pursuing the Ph.D. degree in electrical engineering with the Indian Institute of Technology Kanpur, Kanpur, India. His current research interests include the design of microwave planar sensors for electromagnetic characterization of materials.



Mohammad Jaleel Akhtar (S'99–M'03–SM'09) received the Ph.D/Dr.-Ing. degree in electrical engineering from the Otto-von-Guericke University of Magdeburg, Magdeburg, Germany, in 2003.

From 1994 to 1997, he was a Scientist with the Central Electronics Engineering Research Institute, Pilani, India, where he was mainly involved with the design and development of high-power microwave tubes. From 2003 to 2009, he was a Post-Doctoral Research Scientist and a Project Leader with the Institute for Pulsed Power and Microwave Technology, Karlsruhe Institute of Technology, Karlsruhe, Germany, where he was involved with a number of projects in the field of microwave material processing. In 2009, he joined the Department of Electrical Engineering, Indian Institute of Technology Kanpur, India, where he is currently an Associate Professor. He is the author of two books, two book chapters, and has authored/co-authored over 100 papers in various peer-reviewed international journals and conference proceedings. He also holds one patent on coplanar-based RF sensors. His current research interests include RF, microwave and THz imaging, microwave nondestructive testing, RF sensors, functional materials, wideband electromagnetic absorbers, UWB antennas for imaging, and design of RF filters and components using the electromagnetic inverse scattering.

Dr. Akhtar is a Life Member of the Indian Physics Association and the Indo-French Technical Association. He was a recipient of the CST University Publication Award in 2009 from CST AG, Germany. He served as Chair of the IEEE MTT-S Uttar Pradesh Chapter during 2013–2015, and a Vice-Chair of the IEEE Uttar Pradesh Section during 2015.